Effect of charged-particle bombardment on collector mirror reflectivity in EUV lithography devices

J. P. Allain[1,*], M. Nieto[1], A. Hassanein[1], V. Titov[1], P. Plotkin[1], M. Hendricks[1],
E. Hinson[2], C. Chrobak[3], M.H.L. van der Velden[4], B. Rice[5]

[1]Argonne National Laboratory, Argonne, Illinois
[2]Middlebury College, Middlebury, Vermont
[3]University of Wisconsin, Madison, Wisconsin
[4]Technische Universiteit Eindhoven, Eindhoven, Netherlands
[5]Intel Corporation, Hillsboro, Oregon

ABSTRACT

EUV metallic light radiators such as Sn or Li used for lithography will limit the lifetime of collector optics in source devices by both contamination and irradiation. Generation of EUV light requires the use of hot, dense plasma. Pinch dynamics generates fast ions and atoms, such as metallic sources (Sn, Li) with energies ranging from 100 eV up to several keV. The expanding Sn plasma will thermalize and condense in nearby components, including the debris shield and collector optics. The incident distribution of debris onto the collector optics will likely include Sn fast ions. Sn contamination will lead to two different mechanisms. One is condensation and Sn thin-film buildup on the reflective optics surface (i.e., Ru or Pd mirror) from the thermalized Sn plasma. This mechanism will lead to performance failure after about 1-2 nm build up of Sn thin film whereby the at-wavelength EUV reflectivity will decrease 20% in magnitude for grazing incident angles less than 20-degrees. The second mechanism is more complex. Fast Sn ions generated at the pinch will reach the collector optics and induce mixing, sputtering, and implant at depths between 3 and 5 monolayers on the Ru or Pd surface. EUV light can also induce ionization in background Ar or He gas used for debris mitigation. Low-energy Ar or He ions therefore impinge on the collector mirror surface at threshold-level energies between 40 and 100 eV. A steady-state Sn surface concentration will be attained after a given fluence of both Sn debris and low-energy Ar ions. The amount of Sn implanted or deposited will affect EUV reflectivity as a function of ion and/or atom fluence. Sn contamination mechanisms, as well as threshold-level sputtering from inert ion species, are studied in the IMPACT (Interaction of Materials with charged Particles and Components Testing) experiment. Sn exposure conditions include incident singly charged particles between 500 and 1000 eV, oblique incidence and incident fluxes ranging from 10^{11} to 10^{14} ions/cm^2/s. In-situ surface metrology includes sputter yield diagnosis, Auger electron spectroscopy, X-ray photoelectron spectroscopy, direct recoil spectroscopy and low-energy ion scattering spectroscopy, and at-wavelength EUV reflectivity.

Keywords: threshold sputtering, EUV reflectivity, Sn implantation, Sn deposition, EUV collector optics, ion scattering spectroscopy

1. INTRODUCTION

Energetic charged particle bombardment is one of the key factors leading to reduced lifetime and performance of EUV mirrors by inducing sputtering and/or increasing the roughness of the surface. Two main sources of charged particles have been identified with the potential of damaging the mirror: energetic particles, charged or neutral, coming from the expansion at the end of the pulse of the high-temperature pinched plasma, and low-energy ions from a photo-ionization low-temperature plasma formed around the collector mirror surface.

Extreme ultraviolet lithography (EUVL) tools used in the semiconductor industry utilize 13.5 nm wavelength light. This radiation may generate weakly ionized plasma in the condenser optics region of the tool by photo-ionization of background argon gas. Ions from this plasma get accelerated by the sheath toward the first condenser optic (collector mirror), potentially causing damage through physical sputtering. In addition, low-energy Ar ions can induce physical etching mechanisms, which in synergy with both thermal Sn atoms and energetic fast Sn ions can lead to an equilibrium

kinetic state whereby the EUV reflectivity can be affected. To evaluate the damage to the collector mirror by this mechanism, the sputter yield (atoms removed per incident ion) for argon on ruthenium needs to be measured. Particle-in-cell Monte Carlo simulations have suggested that the Ar ion energy is on the order of tens of eV, well below the typical energies for which experimental data is readily available [1].

More energetic ions can also reach the mirror, generated when the hot temperature plasma pinch collapses and expands. Experiments have measured these ions to have energies of several keV, for both LPP [2] and GDPP [3] sources. The effect of such energetic ions on EUV reflectivity is mainly due to the erosion of material. However, the effect of ions that may get incorporated into the mirror material upon implantation, such as tin, has not received a lot of attention. This work presents the most recent results regarding the effect of Sn bombardment and thermal Sn deposition on the reflectivity of single layer mirrors (SLM) and multilayer mirrors (MLM). In addition, initial measurements of threshold sputtering of Ru by low energy Ar ions are presented.

2. EXPERIMENTAL SETUP

2.1 IMPACT

The Interaction of Materials with Particles and Components Testing (IMPACT) experimental facility was recently built at Argonne National Laboratory (ANL) for measuring and testing charged-particle interactions with multicomponent systems. It is part of the Particle-Radiation Interactions with Matter Experiments (PRIME) facility. Figure 1 presents an internal view of the IMPACT experimental chamber, where base pressures between 10^{-9} and 10^{-8} Torr are routinely achieved.

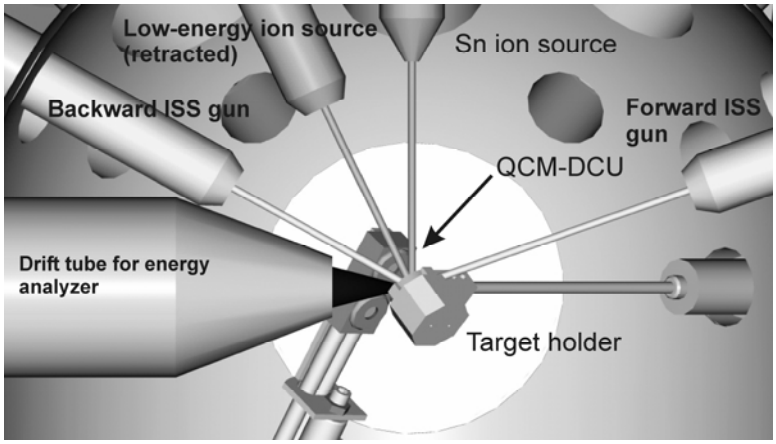

Figure 1: A view inside the IMPACT (Interaction of Materials with charged Particles And Components Testing) experiment at Argonne National Laboratory, showing the relevant components: ion sources, sample holder, energy analyzer, dual QCM unit. Not shown is the 4-pocket electron beam evaporator, also pointing towards the sample holder.

Several in-situ metrology techniques are available for use in the IMPACT chamber. These include low-energy ion scattering spectroscopy (LEISS), Auger electron spectroscopy (AES), X-ray photoelectron spectroscopy (XPS) and extreme ultraviolet photoelectron spectroscopy (EUPS). All these techniques can interrogate the sample during exposure to ion beam bombardment or some other treatment. LEISS gives compositional information about the top monolayer in the sample, while AES and XPS probe the subsurface layers due to deeper probing depths of electrons and x-rays in the material. The techniques complement each and allow a more reliable identification of components as well as their relative abundance and chemical state. In-situ diagnosis of samples monitors dynamic changes that can occur on a surface while it is being irradiated by an ion beam; for example, radiation-induced segregation may drive certain target components to the surface, while radiation-enhanced diffusion will drive them away from the surface. Such phenomena are usually very hard to study by looking at samples before and after the treatment, since the mere act of transporting them to a different chamber for analysis modifies the surface.

2.2 Description of the IMPACT ion sources

As a facility mainly focused in the interaction of ion beams with materials, IMPACT is furnished with multiple ion sources specialized for particular applications or regimes. Three ion gun models manufactured by Nonsequitur Technologies are installed on IMPACT: model 1401, model 1402 and model 14MS. Model 1401 is a standard filament ion source, capable of producing ion currents up to a few μA on spots with a diameter of 0.5 to 1 mm for energies between 500 and 5000 eV. This source is used mainly as the probing beam for the LEISS in-situ technique; it is occasionally used as a sputtering source.

The 1402 source has an optical column optimized for the extraction of low-energy ions with currents on the order of μA for energies between 20 and 1000 eV for all noble gases. This source is particularly useful for the sputtering threshold measurements presented in this work, since having a high-flux, low-energy ion beam allows for the measurement of very low sputtering yields using the QCM-DCU technique implemented on IMPACT. A drawback of this source is that the method employed for beam alignment and size measurement, which uses an oxidized Li foil for imaging based on ion-induced photoemission of the LiI doublet at 670.8 nm, does not work for energies below 150 eV. For such energies, an in-situ current probe is used to measure the spatial variation along one dimension over the target surface. A beam imaging system consisting of an in-situ microchannel plate (MCP) with a luminescent cathode coating will be installed in IMPACT for better ion beam alignment and characterization, especially for the case of the low energy ion source. In addition at lower energies (< 50 eV) an electron bath is applied to stabilize the expanding beam due to the high current densities on the surface during irradiation.

The 14MS source is a metal ion source, currently set to operate with Sn ions. EUV mirrors are exposed to energetic Sn ions to test damage mechanisms to the mirror resulting from heavy-ion bombardment, as well as to study the interaction of the implanted Sn ions with the mirror material/structure. This source also has the advantage of being able to operate with gas if the metal oven is turned off. The source can output a Sn ion current on the 10 to 100 nA range, and with spot sizes between 0.5 and 1 mm. It is also equipped with a Wien filter, which allows the selection of mass and charge of the ions. Figure 2 presents the spatial profile of singly and doubly ionized Sn ions obtained by rastering the beam over an in-situ 5-pinhole Faraday cup.

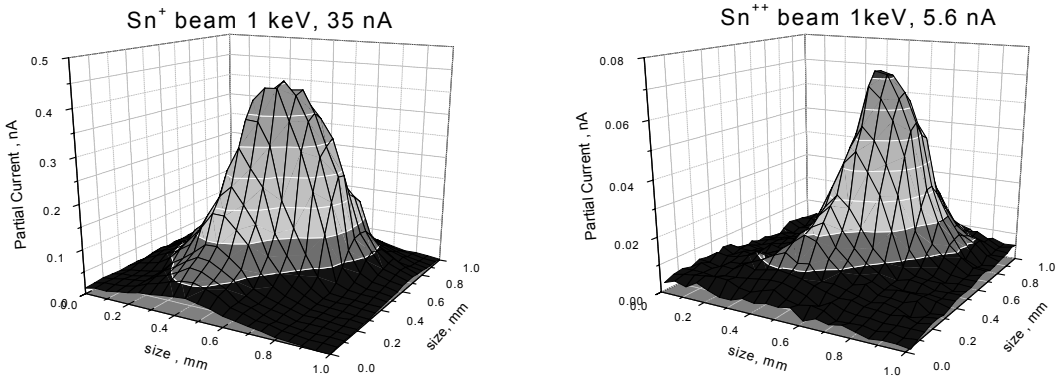

Figure 2: Spatial profiles for Sn^{+} (left) and Sn^{2+} (right) ion beams obtained with the 14MS Sn ion source. The Wien filter selects the ion mass or charge state.

2.3 Description of the in-situ IMPACT EUV reflectometer

Recently, an in-situ EUV reflectometer was added to IMPACT to monitor the relative EUV (13.5 nm ± 0.75 nm) reflectivity temporal evolution as the sample is modified. The IMPACT EUV reflectometer uses an x-ray tube source manufactured by Phoenix X-ray GmbH with a silicon cathode, which emits a broadband spectra centered at about 13.5 nm (corresponding to the 99.3 eV 2p Si transition) with a width of about 1.5-nm. A detailed description of the source is available in the literature [4]. An elliptical Ru mirror focuses the light cone coming out of the source into a millimeter-size spot on the sample surface. When the sample is tilted at 45°, the light cone centerline is incident at 15° with respect to the sample plane, and the specular reflection of this light gets captured by a photodiode, situated also at 15°. A

second photodiode is located in the line of sight of the source, so that when the sample is fully retracted, the total light output of the source can be monitored. This allows monitoring if the output of the source stays constant and allows appropriate corrections to the measurement if this is not the case. The relative reflectivity change is calculated by monitoring the 15° photodiode during the sample treatment (ion bombardment, vapor deposition, or both) and normalizing to the value measured prior to the treatment. If the initial absolute reflectivity of the sample is known, then the absolute reflectivity evolution during the sample modification can be calculated.

3. EXPERIMENTAL RESULTS AND DISCUSSION

3.1 Interaction of Sn vapor and ions with EUV mirrors

Samples in this study were exposed to two kinds of treatment: Sn thermal deposition and Sn implantation. Sn deposition models the effect of Sn vapor from the source condensing on the surface of the collector, whereas Sn implantation simulates the exposure of the condenser mirror to energetic Sn ions coming from the hot plasma pinch. Since IMPACT has both a thermal source (an EGN4 e-beam evaporator from Oxford Applied Research) and an energetic ion source (the 14MS metal ion source from Nonsequitur Technologies), the effect of both Sn exposure types can be evaluated.

Ru samples were exposed to a thermal Sn flux that deposited a 4 to 5 nm thick layer of Sn on top of a Ru mirror. After exposure, measurements of absolute EUV reflectivity were performed at the NIST-SURF facility. The results are shown in Figure 3, for a virgin sample (Ru-108) and the sample exposed to Sn vapor (Ru-106). Overall, approximately 50% reduction in the reflectivity is observed for the wavelength range scanned. The computer simulation of thermal Sn deposition is straightforward since it is equivalent to growing a Sn layer of a given thickness on top of the reflective surface, and good matches can be obtained by setting the layer thickness as a fitting parameter. Along with the measured values, CXRO calculations are also shown in Figure 3, which show that simulating a 2 nm thick Sn layer matches the experimental data very well. This value is also close to the value of about 3-4 nm estimated from the calibration of the IMPACT evaporator. This reflectivity loss as a result of Sn deposition is not exclusive to SLMs at grazing incidence. A reflectivity loss is observed for the case of multilayers exposed to thermal Sn as well, as shown in Figure 4. In this case, the reflectivity drops 33% from the value of the virgin sample compared to the one with Sn deposited in the surface.

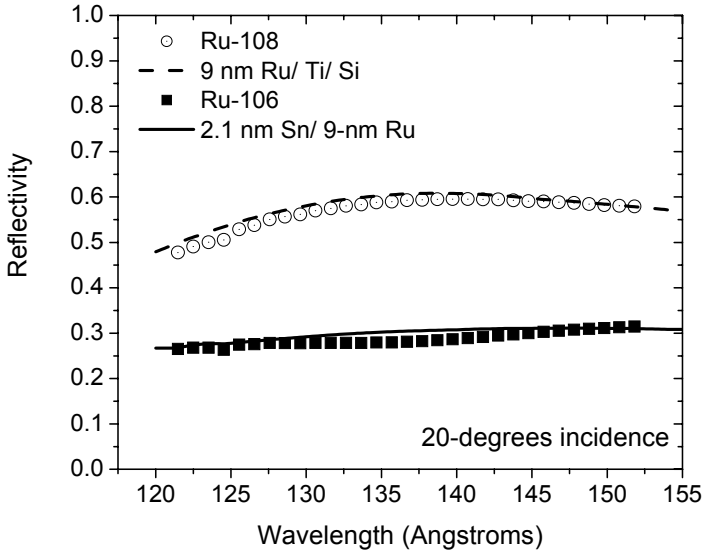

Figure 3: Absolute EUV reflectivity measurement for two Ru mirrors, one unaltered and the other one coated with a 4 nm Sn layer. Measured values are shown with symbols, and solid lines represent results from CXRO calculations. Reflectivity drops roughly 50% for the sample coated with Sn.

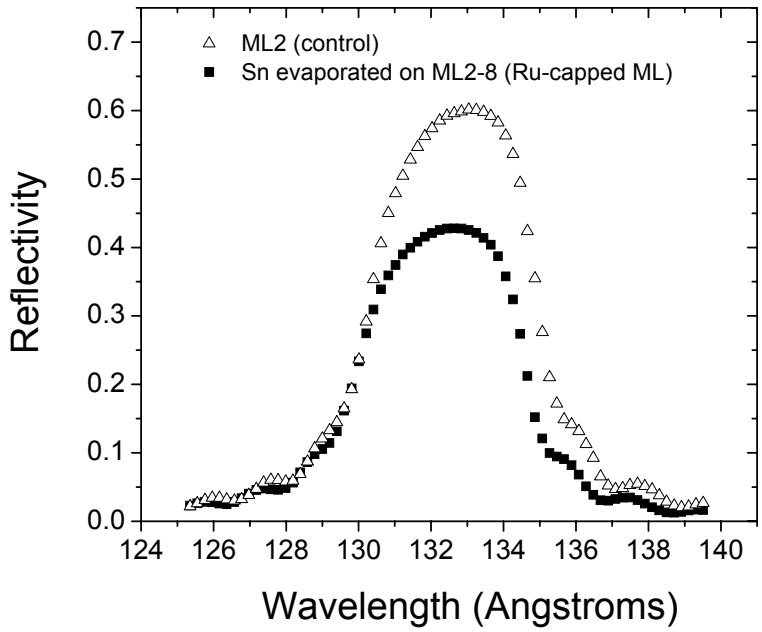

Figure 4: Absolute EUV reflectivity measurement for two Ru-capped multilayered Mo-Si mirrors, one unaltered and the other one coated with a Sn layer. As in the case of the single layer mirror, there is a significant reflectivity drop caused by the presence of Sn in the surface.

The mechanism for reflectivity loss as a result of Sn deposition is well understood and easy to model. In fact, chemical treatments for Sn deposition removal from collector mirrors have been already proposed to mitigate this problem [5]. However, the effect of implanted Sn ions on the reflectivity is not well understood yet, since its implantation on the mirror surface is quite different from thermal condensation. Implantation provides enough energy to break the energy barrier of the air/film interface, and the implants have a much stronger interaction with the mirror material than does a film deposited on the surface. Thus irradiation-driven effects can lead to diffusion of implanted species away from the air/film interface. In addition, enhanced diffusion at grain boundaries can also aid in larger implant mobility on the surface and similarly into the bulk. Currently studies are beginning to define and assess how these mechanisms govern the transport of Sn on both the surface of candidate EUV mirrors and into the film.

Another key difference between thermal and energetic Sn exposure is the ability of the energetic Sn to remove previously implanted Sn. This causes the Sn content to reach an equilibrium state, such that the amount of Sn implanted in the sample equals the amount of Sn leaving the sample as a result of self-sputtering. This can be clearly seen in Figure 5, which shows the evolution of the Sn atomic fraction on the surface measured in IMPACT with time, also indicating the fluence with a solid line. A dose on the order of 10^{16} ions/cm^{-2} results in saturation of the Sn atomic surface fraction based on LEISS data taken during implantation with 1.3 keV Sn ions. For the case of 1 keV incident Sn ions, the saturation content of Sn at the top monolayer is between 45 and 60%, consistent with calculations from the SIBIDET code [6], as shown in Figure 6, where the solid line shows the expected evolution of the Sn surface fraction as calculated by the code and symbols denote the experimental data from Figure 5. After 4 hours of exposure the Sn bombardment stopped, and the fluence remained constant, indicating that no more Sn was injected. Another LEISS scan was taken 80 hours after the Sn bombardment stopped, and a 50% drop in the Sn content at the top 1 ML was observed. This is attributed a diffusive mechanism or surface reconstruction step, however such behavior is still under study and additional experiments are under way to understand this behavior.

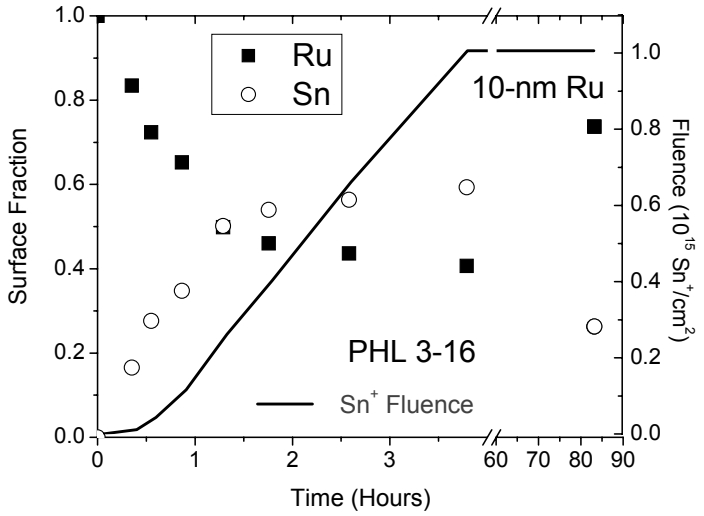

Figure 5: Evolution of the surface composition of a Ru mirror undergoing Sn bombardment at 1 keV and normal incidence. The solid line shows the cumulative Sn dose to the sample, with the scale on the right axis. After many hours, the observed Sn fraction at the surface has dropped 50%.

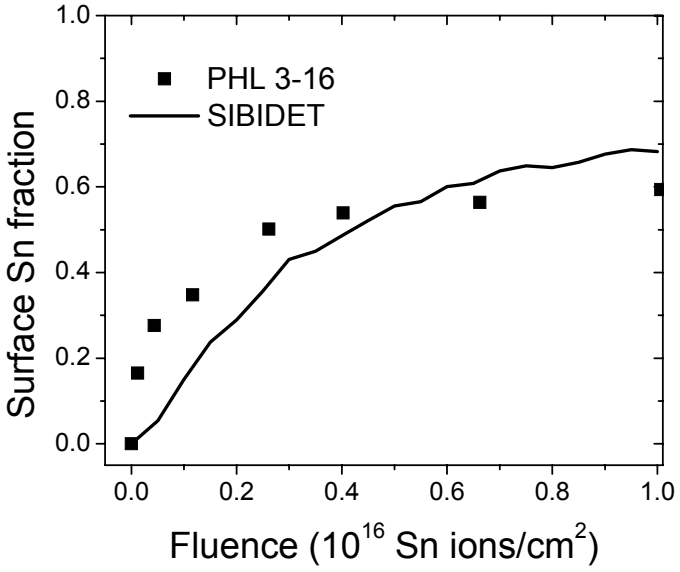

Figure 6: Comparison of the experimental data from Figure 5 with a SIBIDET simulation using the same conditions. The same qualitative response for the Sn content in the surface is observed for both the experiment and the calculation.

3.2 Measurements of threshold sputtering yield of Ru SLM by Ar ions

The EUV radiation generated from the source is able to photoionize some of the background gas in the vicinity of the collector mirror, hence forming a low-temperature plasma. Some of the ions in this plasma may get accelerated by the plasma sheath toward the collector surface and strike it with an energy on the order of tens of eV. In these experiments, aimed to measure sputtering yields of Ru by Ar below 100 eV, a well-defined monoenergetic beam of Ar+ ions bombards a Ru target. The mass of sputtered material is measured by using a quartz crystal microbalance dual-control unit (QCM-DCU), with one crystal facing the target subtending a known solid angle and the other crystal shielded so it can be used as reference [7]. The total mass, Δm_d, of sputtered material deposited on the QCM is defined as

$$m_d = m_{Ru} D S_{QCM} Y C_{fr} , \tag{3.1}$$

where m_{Ru} is the mass of the sputtered particle, D is the ion dose, S_{QCM} is the sticking coefficient, C_{fr} is the fraction of the normalized distribution of sputtered particles subtended by the QCM crystal, and Y is the sputter yield.

The mass deposited on the crystal changes its resonance frequency. The measured variation in the crystal frequency Δf is proportional to the mass deposited on the crystal according to

$$\frac{m_d}{m_{cr}} = \frac{\Delta f}{f} , \tag{3.2}$$

with m_{cr} the mass of a "clean" QCM crystal and f the natural oscillation frequency of the crystal. Therefore, the yield corresponds to

$$Y = \frac{1}{D C_{fr} S_{QCM}} \frac{m_{cr}}{m_{Ru}} \frac{\Delta f}{f} . \tag{3.3}$$

The collected fraction C_{fr} can be calculated by integrating the normalized angular sputter distribution $Y(\theta)$ over the solid angle Ω_{QCM} subtended by the QCM,

$$C_{fr} = \frac{1}{2\pi} \int_{\Omega_{QCM}} Y(\theta) d\Omega \tag{3.4}$$

In the linear cascade regime the projectile ions transfer momentum isotropically to surface atoms of the target material. The probability that these particles will escape to the surface is proportional to the momentum component in the direction normal to the surface. Hence, the angular sputter distribution will show a cosine dependence $Y(\theta) = \cos\theta$. In the single-knock-on regime momentum transfer is no longer isotropic but is more directed in the forward scattering direction. Therefore, the fraction of sputtered particles is greater at lateral angles than at normal angles to the target. As a result, the angular sputter distribution will tend to be under cosine.

When measuring threshold sputtering, the sensitivity of the crystal is critical. Hence, any temperature effect on the crystal needs to be removed, since temperature has a strong effect on the crystal's frequency stability. The relation between the frequency of the crystal and temperature can be approximated by a cubic function, and the frequency stability of the crystal is best near the inflection points of this cubic function. The position of the inflection points is mainly determined by the angle of cut of the crystal relative to the crystallographic axes of quartz, provided no thermal gradients are present. Frequency fluctuations caused by absorption and desorption of background molecules are minimized by measuring the change in the difference between the frequencies of the exposed and background crystals before and after the ion irradiation. To illustrate the technique and the data obtained from it,

Figure 7 shows Ar ion-beam integrated spatial 1-D current profile data for the case of energies below 150 eV used in this study. Figure 8 shows the typical data monitored during a sputtering measurement experiment. The upper panel in Figure 8 shows the frequency evolution of both the reference and exposed crystals; the middle panel shows the frequency difference between the two crystals; and the lower panel shows the ion current and the QCM temperature. The data clearly shows the frequency difference decrease caused by deposition from the sputtered Ru mirror by low-energy Ar ions. During this time the quartz crystal oscillator temperature increased about 5 C. The low-energy ion beam currents achieved were significantly high. For example, at 50 eV incident energy current densities in the order of 10^2 nA/cm^2 were sufficient to erode material for accurate measurement with our QCM-DCU technique.

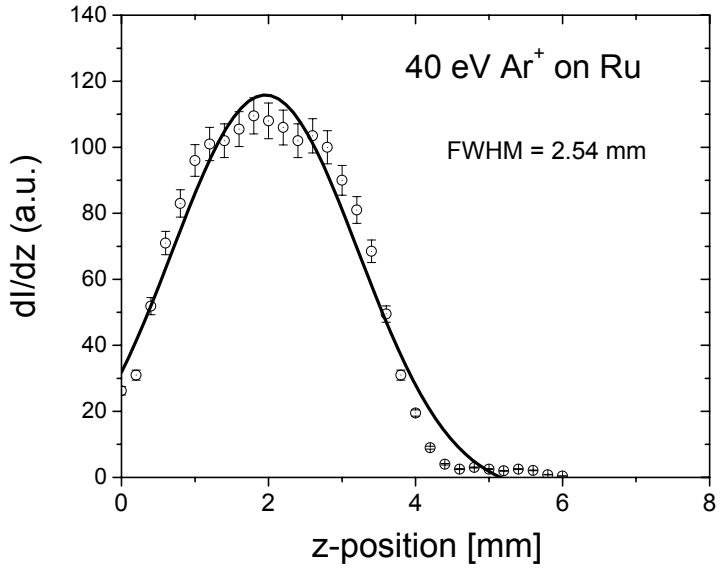

Figure 7: Typical data of Ar ion-beam profiles at energies between 30 and 100 eV.

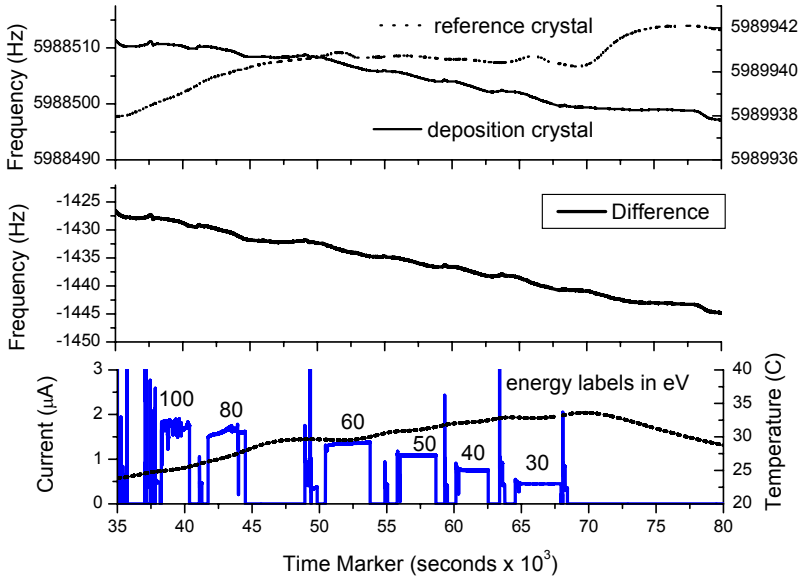

Figure 8: Typical data from threshold sputtering experiments. The frequency of the two QCM crystals is shown in the upper panel, the difference between the two crystals is presented in the middle panel, and sample current and temperature of the QCM holder are shown in the lower panel. A series of irradiations of sample MARC 4 were done with Ar ions at energies between 30 and 100 eV.

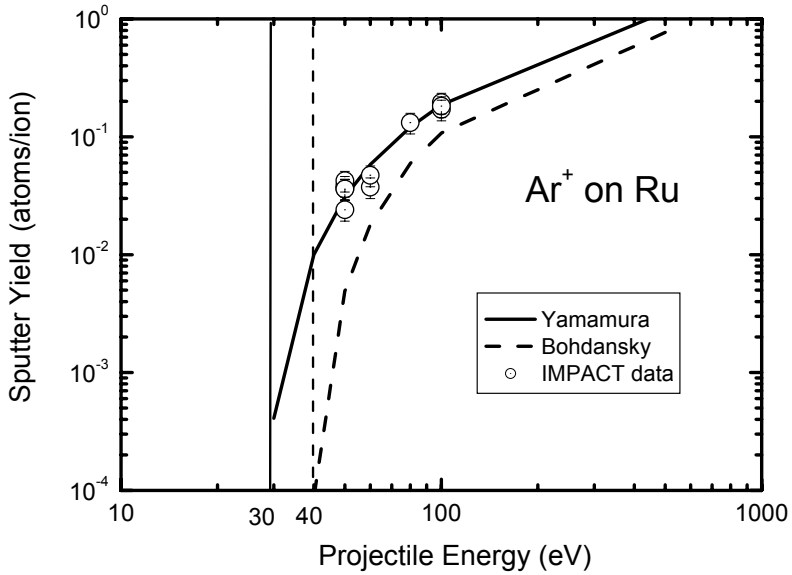

Figure 9: Absolute sputtering yield of Ru near threshold for bombardment with Ar ions at normal incidence. IMPACT data is plotted with semi-empirical models of sputter threshold energies for Ar on Ru by Yamamura and Bohdansky.

Figure 9 shows the absolute sputtering data in the threshold region resulting from low-energy Ar ion bombardment. This data is calculated from the QCM measurement and estimation on the angular sputtered distribution and collected sputtered fraction. The data shows yields near 10% for ~ 100 eV impact energies. At lower energies, sputtering decreases nonlinearly, as predicted by models by Yamamura and Bohdansky [8, 9]. The important result here is that if EUV-induced Ar plasma is generated at the optics, a nontrivial sputtering coefficient will exist at the collector optics surface. The magnitude of this issue and its implications to high-volume manufacturing in future commercial EUV DPP sources need further investigation. In addition, for Sn-based DPP sources the synergy between bombardment by energetic Sn ions from the pinch and low-energy Ar ions induced by the generated EUV light also needs attention; it is currently being studied by our group at Argonne.

4. CONCLUSIONS

Plasma-facing EUV source device materials will need to be carefully designed to handle the harsh environment they will be exposed to. Collector mirror optics materials have been tested in IMPACT under Ar, Sn and Xe ion bombardment. Results for particle bombardment at energies between 100 and 1000 eV show comparable sputter yield magnitudes for Ar, Sn and Xe ions on both Ru and Sn surfaces. Debris mitigation systems using Ar buffer gas, such as an Ar flowing curtain, are needed to slow particles from several keV down below 100 eV to obtain order-of-magnitude reduction in sputtering. Moreover, few sputter capping materials exist for heavy-ion sputtering at these energies, including the use of tungsten or platinum. Although carbon does have substantially lower sputter yield at energies below 100 eV, their active surface with background impurities could be detrimental to EUV reflectivity performance. Current work in IMPACT on assessing the effect of fast ion irradiation under conditions found in EUV sources on in-band EUV reflectivity continue in an upgraded design exploiting in-situ metrology.

5. ACKNOWLEDGMENTS

We acknowledge helpful discussions with U. Stamm, Vadim Banine, T.D. Chinh, J. Pankert and P. Zink. Charlie Tarrio and Stephen Grantham of the NIST-SURF facility are also acknowledged for conducting absolute EUV at-wavelength measurements of the Ru grazing incidence mirror samples irradiated and exposed at Argonne National Laboratory. Peter Loeffler from Nonsequitur Technologies in Bend, Oregon for his steadfast technical support on our ion sources; in particular the Sn metal-ion source currently under development between NTI and ANL. This work was supported by Intel Corporation and in part by the U.S. Department of Energy under Contract W-31-109-Eng-38.

6. REFERENCES

1. N.Matsunami, Y.Yamamura, Y.Itikawa et.al., *Institute of Plasma Physics. Nagoya University Japan, Report No. IPPJ-AM-32* (1983).
2. Akira Endo, IEEE Journal of Selected Topics in Quantum Electronics **10**, (2004) 1298.
3. Erick L. Antonsen *et al.*, *XCEED: XTREME commercial EUV exposure diagnostic experiment*, presented at the SPIE: Emerging Lithographic Technologies IX, San Jose, CA, 2005, Vol 5751, 1211.
4. A. Egbert, B. Mader *et al*, Journal of Microlithography, Microfabrication, and Microsystems **2**, (2003) 136.
5. J. Pankert et al., "Integrating Philips' extreme UV source in the alpha-tools", Proc. SPIE Int. Soc. Opt. Eng. 5751 (2005) 260
6. Jean P. Allain *et al.*, *Erosion and degradation of EUV lithography collector mirrors under particle bombardment*, presented at the SPIE: Emerging Lithographic Technologies IX, San Jose, CA, 2005, Vol 5751, 1110.
7. J.P. Allain and David N. Ruzic, Nuclear Fusion **42** (2002) 202.
8. J.Bohdansky, Nuclear Instrumentation and Methods B **2** (1984) 587.
9. Y.Yamamura and H.Tawara, Atomic Data and Nuclear Data Tables. **62** (1996) 149.